2-μm wavelength, high-energy Ho:YLF chirped-pulse amplifier for mid-infrared OPCPA

M. Hemmer,[1,*] D. Sánchez,[1] M. Jelínek,[2] Vadim Smirnov,[3] H. Jelinkova,[2] V. Kubeček,[2] and J. Biegert[1,4]

[1]*ICFO—Institut de Ciencies Fotoniques, Mediterranean Technology Park, Castelldefels, Barcelona, Spain*

[2]*Czech Technical University in Prague, Faculty of Nuclear Science and Physical Engineering, Brehová 7, 11519 Prague 1, Czech Republic*

[3]*OptiGrate Corparation, 562 S. Econ Circle, Oviedo, Florida 32765, USA*

[4]*ICREA—Institució Catalana de Recerca i Estudis Avançats, Barcelona, Spain*

**Corresponding author: michael.hemmer@icfo.eu*

Received November 7, 2014; accepted December 20, 2014;
posted December 23, 2014 (Doc. ID 226450); published February 2, 2015

A 2-μm wavelength laser delivering up to 39-mJ energy, ~10 ps duration pulses at 100-Hz repetition rate is reported. The system relies on chirped pulse amplification (CPA): a modelocked Er:Tm:Ho fiber-seeder is followed by a Ho:YLF-based regenerative amplifier and a cryogenically cooled Ho:YLF single pass amplifier. Stretching and compressing are performed with large aperture chirped volume Bragg gratings (CVBG). At a peak power of 3.3 GW, the stability was <1% rms over 1 h, confirming high suitability for OPCPA and extreme nonlinear optics applications.

OCIS codes: (140.5680) Rare earth and transition metal solid-state lasers; (140.3280) Laser amplifiers.
http://dx.doi.org/10.1364/OL.40.000451

Intense ultrafast sources in the mid-IR are highly attractive [1] since they enable exploiting nonlinear optics in the anomalous dispersion regime that can lead to clean self-compression directly to the few-cycle regime [2] or extreme supercontinuum generation [3–5]. These sources permit rapid identification of volatiles in the molecular fingerprint region [6,7] without arduous scanning and are attractive for military applications and to drive strong field physics experiments [8,9]. Optical parametric chirped-pulse amplification (OPCPA) has emerged as a powerful technique for the generation of high-power [10] and high-energy [11] ultra-short mid-IR pulses, but further progress is hampered by the near exclusive usage of ~1 μm pump lasers. These pump lasers impose an unfavorable photon ratio between pump and signal/idler that limits efficiency, prevents accessing the highly efficient class of non-oxide crystals, and presents serious power scaling limitations due to linear and two-photon absorption [12]. These limitations can be mitigated using powerful pump lasers emitting at 2-μm wavelength thereby reducing the photon ratio mismatch and allowing the use of highly nonlinear non-oxide crystals such as ZGP [13]. While the technology of such lasers, based on *Q*-switched Ho:YLF (or Ho:LuLiF) and Ho:YAG, is very mature for generating high-energy nanosecond pulses [14–20], amplification of few picosecond pulses from such systems to the multi-tens of mJ has not been reported.

In this Letter, we report on a compact and stable laser system operating at 2-μm wavelength, delivering ~10 ps duration optical pulses with up to 39-mJ output energy at 100-Hz repetition rate. Highly efficient temporal compression of narrow-band picosecond pulses was performed at the multi-tens of mJ energy-level in a chirped volume Bragg grating (CVBG).

The laser system relies on chirped pulse amplification (CPA) architecture consisting of a fiber seeder, a CVBG stretcher, two consecutive amplification stages, and a large aperture CVBG compressor (Fig. 1). The all-fiber seeder is a multi-stage system (Menlo Systems GmbH) starting with an amplified modelocked Er:fiber oscillator delivering femtosecond optical pulses at 100-MHz repetition rate and 1.5-μm wavelength. These pulses are frequency shifted to 2052-nm wavelength and spectrally narrowed to ~1.5 nm bandwidth before seeding a series of Tm:Ho fiber amplifiers [21]. The 4-nJ energy, picosecond duration pulses emerging from these amplifiers at 100 MHz form the seed for the CPA chain thereby removing the problem of modelocking Ho-based systems directly. These pulses are temporally stretched to 170-ps duration in a double-pass, CVBG-based stretcher. The CVBG (OptiGrate Corp.) used in this stretcher is broadband AR-coated around 2052 nm, has a 5 mm × 8 mm clear aperture, a chirp rate of 150 ps/nm, and a design wavelength of 2053.5 nm. Upon stretching, the 100-MHz train is passed through a rubidium titanyle phosphate (RTP) pulse picker to reduce the repetition rate to 100 Hz. The pulses are then passed through an optical isolator and directed toward a regenerative amplifier. The quasi-three-level Ho:YLF crystal was chosen as gain medium for the regenerative amplifier since it exhibits one of the highest emission cross-sections for rare-earth-doped materials with emission in the 2050-nm spectral region, a long excited-state lifetime particularly desirable for amplification to high energy at low repetition rate and favorable thermo-optical properties, in particular natural birefringence and weak thermal lens [15,16,22].

A 3.5-cm-long, 0.5% doped Ho:YLF crystal mounted in a water-cooled copper mount is used as gain medium in this amplifier. The length and dopant concentration of the crystal were determined via numerical simulations to strike a balance between optimum pump absorption and gain. The pump energy is provided by a commercial Tm:fiber laser (IPG Photonics) delivering up to 30 W of continuous wave (CW) unpolarized output at 1940 nm. The pump was passed through a polarizer to ensure pumping with π-polarization, while the c-axis of the crystal was aligned horizontal and the pump propagating

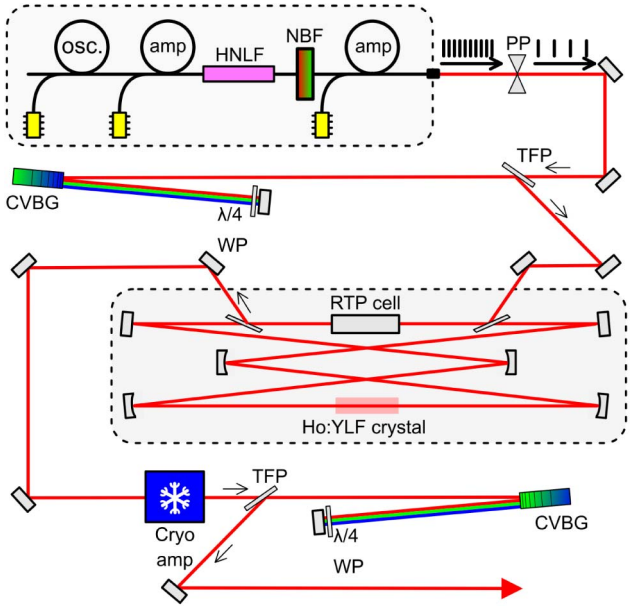

Fig. 1. Layout of the 2-μm CPA system featuring a fiber seeder, CVBG-based stretcher, ring regenerative amplifier, cryogenically cooled single-pass amplifier, and CVBG-based compressor. HNLF, highly nonlinear fiber; NBF, narrow band filter; PP, pulse picker; CVBG, chirped volume Bragg grating; WP, waveplate; TFP, thin-film polarizer.

along the a-axis. We opted for a ring cavity design to guarantee the absence of feedback from the regenerative amplifier into the fiber laser seeder. The seed pulses are injected into and ejected from the amplifier using a combination of thin-film polarizers and an RTP Pockels cell operated at half-wave voltage. The nJ seed pulses are amplified to the 4-mJ level after 36 passes through the gain medium at a CW pump power of ~9.2 W (Fig. 2). Increasing the pump power resulted in a linear increase of the output energy and up to 5.5 mJ could be obtained without damage to any components. We nonetheless chose to operate the regenerative amplifier in a regime where the peak intensity on the intra-cavity optical components was kept below 5 GW/cm^2 and therefore limit the output energy to ~4 mJ. The spatial profile at the output of the regenerative amplifier is Gaussian (Fig. 2—inset) owing to the excellent spatial profile of the pump laser and the quasi-three-level nature of the gain medium that prevents the amplification of higher order transverse modes.

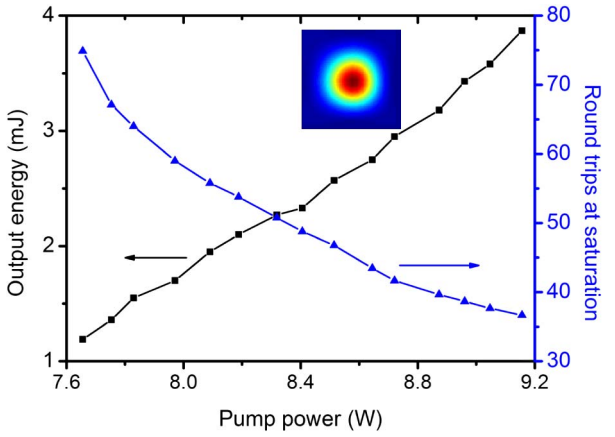

Fig. 2. Measured output energy (black square) and number of passes required to reach saturation (blue triangle) of the Ho:YLF regenerative amplifier. Measured spatial profile at the output of the amplifier (inset).

The power and peak-to-peak fluctuations—recorded, respectively, with a power meter and a fast photodiode—at the output of the regenerative amplifier were measured to be less than 2% rms over 2 h, and performances were reproducible—alignment free—from day-to-day.

Further amplification to much higher pulse energy in multipass geometries would be very challenging with Ho:YLF due to its quasi-three-level nature that results in low gain, high threshold, and unwanted thermal loading [15,16]. The quasi-three-level nature of the crystal nonetheless suggests that under sufficient cooling, the ground state and the lower laser level can separate and allow four-level operation. This concept was exploited recently in a cryogenically cooled Q-switched oscillator, delivering 550 mJ at 1-Hz repetition rate [14]. Thus we investigated the transition point between three- and four-level operation to corroborate whether the temperatures reachable by Peltier cooling would present a practical alternative or the low temperatures only enabled by cryogenic cooling would be necessary. Figure 3 shows the result of our measurement in which we record the evolution of the absorption cross-section of Ho:YLF at the emission wavelength as a function of temperature. The measurement confirms the transition from three- to four-level behavior of the crystal through disappearance of the absorption peak at the emission wavelength, but only at liquid nitrogen temperatures.

Based on these measurements, a single pass, cryogenically cooled Ho:YLF amplifier was built to further boost the energy from the regenerative amplifier. The cooling was provided by a closed-loop Gifford–McMahon-type cryogenic cooler with a cooling capacity exceeding 50 W at liquid nitrogen temperature. A 5-cm-long, 1% doped Ho:YLF crystal was mounted inside a small vacuum chamber onto the cold finger with a cut and orientation identical to those implemented in the regenerative amplifier.

The pump power was provided by a commercial continuous-wave Tm:fiber laser (IPG Photonics) that

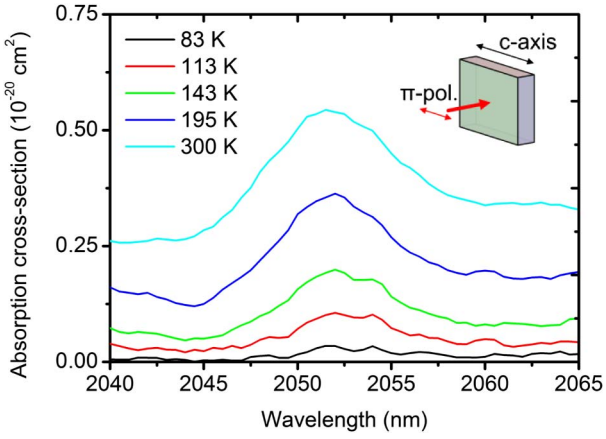

Fig. 3. Measured absorption cross-section of Ho:YLF at the emission wavelength as a function of temperature. Measurements were performed using a 5-mm-thick, 0.5 at. % doped sample. The incoming light polarization was along the c-axis of the crystal and propagation along the a-axis.

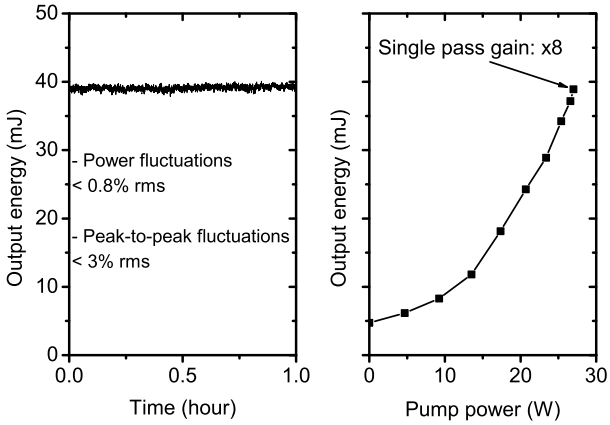

Fig. 4. Measured power stability at the output of the single pass cryogenically Ho:YLF amplifier showing power fluctuations less than 0.8% rms over an hour (left) and characteristics of the amplifier for a seed energy of 4.9 mJ showing 8× single pass gain.

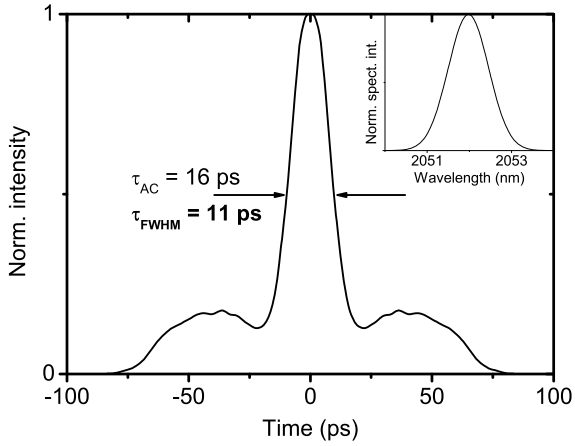

Fig. 5. Measured intensity autocorrelation trace of the compressed pulse. We measure a 16-ps FWHM autocorrelation that corresponds to ~11 ps FWHM. The side lobes are due to uncompensated chirp due to slight mismatch of the stretcher and compressor CVBGs. Inset: measured spectrum after amplification.

delivered up to 120 W of unpolarized power. The pump beam was passed through a polarizer upon exiting the fiber to ensure a polarized pump beam. At a pump power of ~27 W, a single pass gain of 8 could be achieved that resulted—upon seeding 4.9-mJ energy pulses—in an output energy of 39 mJ while maintaining the peak intensity below 5 GW/cm^2. The stability of the output energy was characterized over an hour and revealed excellent performance. We measured power fluctuations less than 0.8% rms and peak-to-peak fluctuations over half a million shots less than 3% (Fig. 4). The spatial profile was left unaffected by the amplification process, owing to the excellent spatial profile of the pump. The pump power was not further increased as the onset of spatial gain narrowing became noticeable. Upon amplification our high-energy pulses were directed toward a CVBG-based pulse compressor.

Progresses in the fabrication of photo-thermo-refractive (PTR) glass have enabled increased uniformity of the refractive index and photosensitivity in CVBGs. These progresses now allow the production of gratings with extended thickness and clear aperture, able to handle high energies while leaving the spatial profile undisturbed. The unique CVBG (OptiGrate Corp.) used in this setup had a 25×27 mm^2 clear aperture, a 40-mm thickness, and was AR-coated on both facets to prevent Fresnel reflections. This CVBG was dimensioned to handle energies up to 50 mJ without suffering from the onset of self-phase modulation, typically observed for peak powers in the 6×10^{12} W/cm^2 range in PTR glass. The CVBG was recorded in wafers showing a refractive index uniformity better than 100 ppm, and the high efficiency of the grating was guaranteed by development of the holographically recorded grating at 500°C.

The CVBG used in the compressor had a design wavelength of 2053.3 nm and a chirp rate of 150 ps/nm, matching that of the stretcher CVBG. Similarly to the stretcher, the compressor was operated in a double-pass configuration. The overall efficiency of the compressor was as high as 85%, and the footprint of the assembly was as small as 50 cm × 10 cm. Figure 5 shows the result from an intensity autocorrelation measurement. The pulse duration at the output of the compressor was 11 ps. Due to the separate manufacturing of the stretcher and large area compressor CVBGs, a slight mismatch existed that can be removed entirely with two identically manufactured future CVBGs. The current mismatch explains the satellites in the temporal trace (Fig. 5) and the departure from the 5-ps transform limit. Nevertheless, for comparison, a standard Treacy compressor relying on off-the-shelf commercial diffraction gratings (600 l/mm) was built and delivered similar pulse duration with a much lower overall throughput of only 10% and a footprint of 180 cm × 70 cm.

These differences in footprint and efficiency highlight the superiority of CVBG solution for compressing narrowband picosecond pulses.

In conclusion, we report on a novel Ho:YLF CPA system delivering narrowband, 10-ps duration, scalable output in the tens of mJ range at 100-Hz repetition rate. These operating parameters were achieved with a compact modelocked Er:Tm:Ho fiber seeder, cryogenic cooling of the gain medium, and a high-efficiency, high-aperture CVBG. Future work will be concerned with further energy scaling to the multi-100-millijoule range and application for direct pumping of mid-IR OPCPA.

This work was supported by Fundacio Cellex Barcelona, the MINISTERIO DE ECONOMIA Y COMPETITIVIDAD through Plan Nacional (FIS2011-30465-C02-01), the Catalan Agen-cia de Gestió d'Ajuts Universitaris i de Recerca (AGAUR) with SGR 2014-2016, LASERLAB-EUROPE grant agreement 284464 and the Czech Science Foundation project P102/13/8888.

References

1. J. Biegert, P. K. Bates, and O. Chalus, IEEE J. Sel. Top. Quantum Electron. **18**, 531 (2012).
2. M. Hemmer, M. Baudisch, A. Thai, A. Couairon, and J. Biegert, Opt. Express **21**, 28095 (2013).
3. F. Silva, D. R. Austin, A. Thai, M. Baudisch, M. Hemmer, D. Faccio, A. Couairon, and J. Biegert, Nat. Commun. **3**, 1 (2011).

4. C. Petersen-Rosenberg, U. Møller, I. Kubat, B. Zhou, S. Dupont, J. Ramsay, T. Benson, S. Sujecki, N. Abdel-Moneim, Z. Tang, D. Furniss, A. Seddon, and O. Bang, Nat. Photonics **8**, 830 (2014).
5. D. D. Hudson, M. Baudisch, D. Werdehausen, B. J. Eggleton, and J. Biegert, Opt. Lett. **39**, 5752 (2014).
6. F. K. Tittel, D. Richter, and A. Fried, Top. Appl. Phys. **89**, 458 (2003).
7. W. Petrich, Appl. Spectrosc. Rev. **36**, 181 (2001).
8. T. Popmintchev, M. Chen, D. Popmintchev, P. Arpin, S. Brown, S. Alisauskas, G. Andriukaitis, T. Balciunas, A. D. Mücke, A. Pugzlys, A. Baltuska, B. Shim, S. E. Schrauth, A. Gaeta, C. Hernandez-Garcia, L. Plaja, A. Becker, A. Jaron-Becker, M. M. Murnane, and H. C. Kapteyn, Science **336**, 1287 (2012).
9. J. Dura, N. Camus, A. Thai, A. Britz, M. Hemmer, M. Baudisch, A. Senftleben, C. D. Schröter, J. Ullrich, R. Moshammer, and J. Biegert, Sci. Rep. **3**, 2675 (2013).
10. M. Hemmer, A. Thai, M. Baudisch, H. Ishizuki, T. Taira, and J. Biegert, Chin. Opt. Lett. **11**, 013202 (2013).
11. G. Andriukaitis, T. Balciunas, S. Alisauskas, A. Pugzlys, A. Baltuska, T. Popmintchev, M. Chen, M. Murnane, and H. Kapteyn, Opt. Lett. **36**, 2755 (2011).
12. M. Baudisch, M. Hemmer, H. Pires, and J. Biegert, Opt. Lett. **39**, 5802 (2014).
13. G. D. Boyd, E. Buehler, and F. G. Storz, Appl. Phys. Lett. **18**, 301 (1971).
14. H. Fonnum, E. Lippert, and M. W. Haakestad, Opt. Lett. **38**, 1884 (2013).
15. W. Koen, C. Bollig, H. Strauss, M. Schellhorn, C. Jacobs, and M. J. D. Esser, Appl. Phys. B **99**, 101 (2010).
16. A. Dergachev, in *Solid State Lasers XXII: Technology and Devices* (2013), Vol. **8599**, p. 85990B .
17. H. J. Strauss, W. Koen, C. Bollig, M. J. D. Esser, C. Jacobs, O. J. P. Collett, and D. R. Preussler, Opt. Express **19**, 13974 (2011).
18. H. J. Strauss, D. Preussler, M. J. D. Esser, W. Koen, C. Jacobs, O. J. P. Collett, and C. Bollig, Opt. Lett. **38**, 1022 (2013).
19. J. Kwiatkowski, J. K. Jabczynski, and W. Zendzian, Opt. Laser Technol. **67**, 93 (2015).
20. M. Schellhorn, Opt. Lett. **35**, 2609 (2010).
21. H. Hoogland, A. Thai, D. Sanchez, S. L. Cousin, M. Hemmer, M. Engelbrecht, J. Biegert, and R. Holzwarth, Opt. Express **21**, 31390 (2013).
22. M. Eichhorn, Appl. Phys. B **93**, 269 (2008).